Pulmonary Nodule Detection, Characterization, and Management With Multidetector Computed Tomography

Scott Brandman, MD and Jane P. Ko, MD

Abstract: Pulmonary nodule detection and characterization continue to improve with technological advancements. The noninvasive methods available for assisting in nodule detection and for characterizing nodules as benign, malignant, or indeterminate will be discussed. Evidence-based guidelines will be reviewed to help guide the appropriate management of pulmonary nodules.

Key Words: pulmonary nodule, computer-aided diagnosis, volume, dual energy, management

(*J Thorac Imaging* 2011;26:90–105)

The solitary pulmonary nodule (SPN) is a frequently encountered finding on multidetector computed tomography (MDCT). A nodule is of high clinical importance, given it may prove to be an early manifestation of lung cancer, which is the leading cause of death in the United States from malignancy.[1] Early detection, accurate characterization, and appropriate management of pulmonary nodules require expertise across multiple disciplines such as radiology, oncology, pulmonary medicine, radiation oncology, and thoracic surgery. Given the high number of SPNs detected on CT and the low sensitivity of both 18F-flourodeoxyglucose (FDG) positron-emission tomography (PET) and CT-guided biopsy for nodules smaller than 5 mm in size, the latest technologies for nodule detection, means of characterizing these lesions, and guidelines for managing lung nodules will be addressed.[2] We will also discuss the role of new and developing technologies, including computer-aided detection (CAD), the nodule volume assessment technique, dual-energy CT, and nodule enhancement.

PULMONARY NODULE DETECTION ON CT

Chest radiography remains the most commonly ordered radiological examination. Unfortunately, radiography has low sensitivity for demonstrating significant lesions and a high false-positive rate for the detection of pulmonary nodules.[3,4] The greater degree of spatial and contrast resolution provided by MDCT enables improved sensitivity and specificity for pulmonary nodule detection. Nevertheless, pulmonary nodules are still undetected on MDCT due to their small size; low Hounsfield unit (HU) attenuation (ground-glass nodules); perivascular central or endobronchial location; or adjacent parenchymal disease.[5–8]

From the Department of Radiology, Division of Thoracic Imaging, New York University Langone Medical Center, New York, NY.
Disclosures: None.
Reprints: Jane P. Ko, MD, Department of Radiology, Thoracic Imaging, New York University Langone Medical Center, 560 First Avenue, New York, NY 10016 (e-mail: jane.ko@nyumc.org).

VIEWING OPTIONS

The widespread availability of MDCT scanners provides the opportunity to examine thin-section (1 mm) CT images in the order of 2 mm and smaller in thickness, which improves reader detection of focal lung findings and characterization of these findings as nodules. The overall sensitivity for reader detection of pulmonary nodules has been reported to be 70% to 75%. However, sensitivity is significantly lower for smaller pulmonary nodules related to volume averaging.[9,10] Diederich et al[10] reported that reader sensitivity using 5-mm sections was 69% for nodules smaller than 6 mm, and 95% for those that were 6 mm or larger. However, the number of images to be examined increases by 5-fold when 1-mm-section images are used instead of 5-mm-section images, which can contribute to reader fatigue.[11] In addition, on thin sections, small pulmonary nodules are difficult to differentiate from normal vascular structures.

Postprocessing techniques are now widely available and can increase reader sensitivity for pulmonary nodules. The maximum intensity projection (MIP) technique displays the brightest voxel along an array within a slab. In the lung, the voxels of a vessel are the brightest (in contrast to the surrounding air-filled acini), and therefore their values are most often used for display. This leads to visualization of the branching vessel within a slab and facilitates differentiation of a perivascular nodule from the vessel (Fig. 1). MIP techniques were shown to improve the visualization of small nodules.[12,13] Park et al[14] reported the nodule detection sensitivities of 4 readers (A, B, C, and D), who interpreted 1-mm sections, as 91%, 88%, 87%, and 86%, respectively. The sensitivities increased to 94%, 96%, 91%, and 92%, respectively, when the readers evaluated 5-mm MIPs reconstructed at 1-mm intervals; the sensitivity change was significant for readers B, C, and D. The value of MIPs has been shown in both axial and coronal projections, in addition to coronal multiplanar reformations.[15] Minimum intensity projection images may potentially play a role in the detection of ground-glass lesions (Fig. 2).

CAD

Computer-assisted image analysis methods can aid the radiologist in detecting lung nodules. These computer algorithms have been enabled by high-resolution thin-section MDCT data. CAD techniques have been shown to increase the detection of small pulmonary nodules while maintaining time efficiency for diagnosis. CAD devices for nodule identification have been primarily investigated in the role of a second reader, in which CAD identifications are viewed subsequent to an initial review by the radiologist.[16–20] For example, in a study by Rubin et al,[17] a CAD device increased reader sensitivity for the detection of pulmonary nodules from 50% to 76%, with 3 false-positive

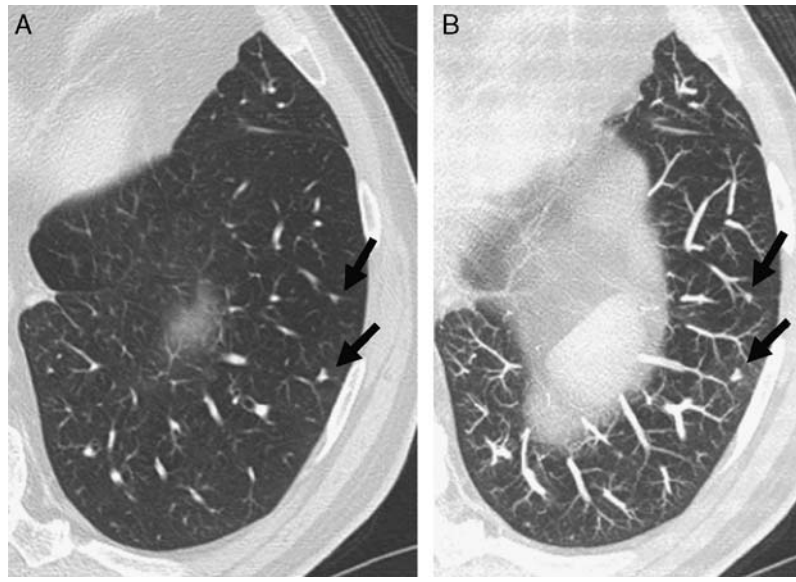

FIGURE 1. MIP image for solid nodule detection. Nodules (arrows) on 1-mm (A) axial section are more evident on the MIP (B) image and are more readily differentiated from the vessels. The courses of the vessels are depicted to a greater degree on the MIP.

detections per CT scan if all the true-positive CAD marks were to be accepted by readers. False-positive detections by CAD were related to artifact, branching points of vessels, or central vessels, and have been reduced with improved CAD schemes to 3 or fewer per CT scan.[17] The maintenance of a low false-positive rate is important, as radiologist confidence in detecting small pulmonary nodules can be influenced by CAD.[21] A recent study demonstrated that a radiologist will accept 11% of false-positive CAD marks.[21] Both CAD and MIP were shown to assist the detection of lung nodules to equal degrees.[14] The utilization of CAD will be facilitated by seamless viewing of CAD results on clinical picture archiving and communication systems (PACS) rather than on a stand-alone workstation, and by ultimately, real-time interaction with CAD results on PACS (Fig. 3).

Minimal investigation has been devoted towards CAD identification of ground-glass nodules.[22–26] CAD detection of ground-glass nodules is difficult. The faint attenuation and low contrast of ground-glass nodules relative to the adjacent lung parenchyma hinder thresholding and segmentation techniques. For example, the sensitivity of a single CAD technique was only 53% for ground-glass nodules, whereas it was 73% for a mixed ground-glass and solid nodule.[27] As this technology continues to evolve, potential exists for devices to positively impact reader detection of lung nodules for both ground-glass and solid attenuation nodules.

Nodule-detection techniques are also needed for automated matching of lung nodules on multiple chest CT studies, an essential aspect of nodule characterization. The process of both nodule detection and image registration requires lung segmentation, feature extraction, and characterization by CAD. The comparison of multiple CT studies poses challenges given variations in inspiratory lung volumes, patient positioning, and lung pathology. Registration techniques to overcome these challenges include rigid methods that account for patient rotation and location of the patient's thorax within the image; however, differences related to scale and changes in lung, lobe, and locoregional morphology that frequently occur are better addressed with deformable models and elastic registration techniques.[28,29] Similar methods are used for intermodality registration, such as CT with magnetic resonance imaging. A study by Tao et al[30] evaluated a computer registration program's ability to automatically match pulmonary nodules on 3 serial screening MDCTs. They demonstrated a 92.7% matching rate between studies performed 1 year apart. Automated matching was not significantly affected by nodule size or ground-glass attenuation. However, a juxtapleural location significantly decreased the matching rate to almost 86%. Other studies evaluated patients with metastatic disease on serial examinations. These studies demonstrated matching rates of only 66.7% and 86.3%.[31,32] Advances in the development of interfaces with clinical workstations would facilitate detection and comparison of nodules over multiple studies in clinical practice.

NODULE MORPHOLOGY ON MDCT AND ETIOLOGIES

Benign nodules result primarily from infection. Infectious granulomas account for more than 80% of benign SPNs[33] (Fig. 4) with mycobacterial infection the most common cause, followed by fungal organisms. Hamartomas, consisting of multiple mesenchymal tissue histologies, represent 10% of benign SPNs.[33] Arteriovenous malformations and aneurysms are other causes of an SPN.

Malignant etiologies for SPNs include primary lung cancer (84%) and solitary metastasis (8%) (Table 1).[34] CT trials for lung cancer screening have found an 8% to 51% prevalence of SPNs in high-risk patients.[35,36] The most common histologic subtype of lung cancer is adenocarcinoma. Adenocarcinoma represents 50% of malignant pulmonary nodules and is typically peripheral in location.[34] Squamous cell carcinoma is the second most common histologic subtype of lung cancer, and two-thirds of these tumors are located centrally.[37] Other subtypes of lung carcinoma can also present as SPNs. Small cell carcinoma

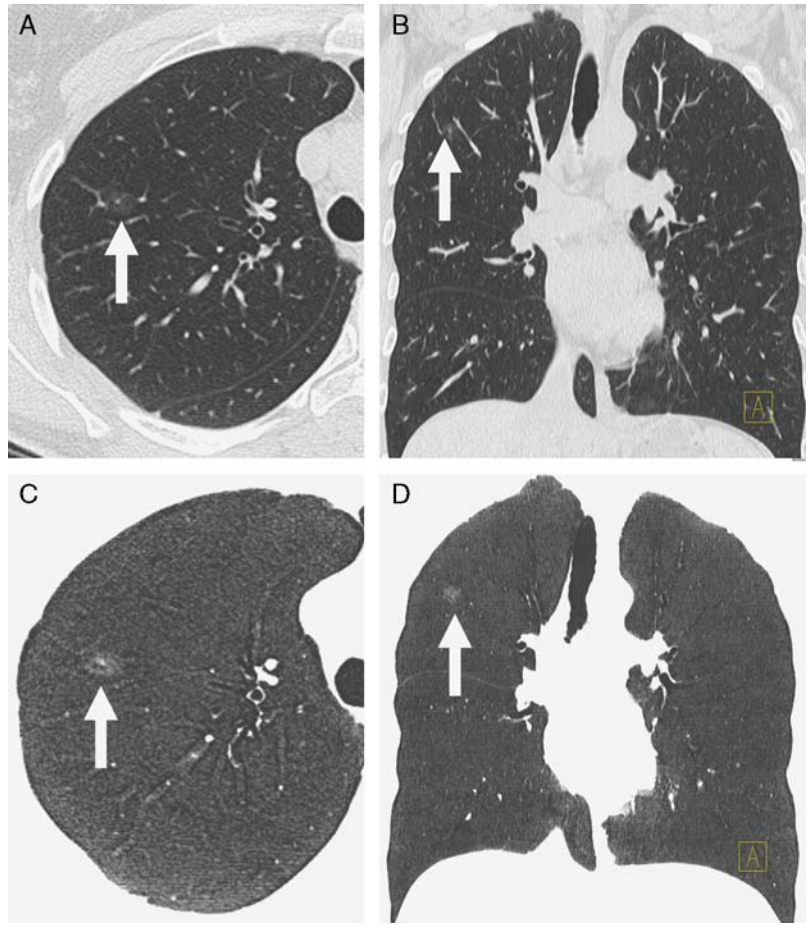

FIGURE 2. Ground-glass nodule (arrows) detection. Axial (A) and coronal 1-mm (B) sections demonstrate a right upper lobe faint ground-glass nodule. Axial (C) and coronal 1-mm (D) minimum intensity projection images increase the conspicuity of the nodule.

occurs as an SPN approximately 5% of the time and more often presents with bulky lymphadenopathy in the hilar and mediastinal regions.[37,38] Carcinoid tumors are neuroendocrine tumors that represent 1% to 2% of all lung tumors, with 10% to 20% atypical and the remainder typical. In addition, 16% to 40% of carcinoids occur in the peripheral lung (Fig. 5).[39,40] Although most often multiple, metastases to the lung parenchyma from an extrapulmonary primary malignancy such as colon and renal cell carcinoma, testicular cancer, melanoma, and sarcoma can appear as SPNs. Lymphoma in the lung parenchyma has several appearances, including that of an SPN (Fig. 6).

Size is a primary factor in determining the risk for malignancy of a nodule. In a meta-analysis of 8 large screening trials, the prevalence of malignancy depended on the size of the nodules, ranging from 0% to 1% for nodules 5 mm or smaller, 6% to 28% for those between 5 and 10 mm, and 64% to 82% for nodules 20 mm or larger.[35]

The presence of multiple nodules increases the likelihood of etiologies such as metastatic disease, septic emboli, and pulmonary infarcts. In addition, inflammatory diseases such as Antineutrophil cytoplasmic autoantibody (ANCA)-associated vasculitis, sarcoidosis, amyloidosis, and rheumatoid arthritis can lead to multiple benign pulmonary nodules.[41,42] Multiple arteriovenous malformations (AVMs) can occur in patients who have hereditary hemorrhagic telangectasias (Osler-Weber-Rendu syndrome). This is autosomal-dominant disease with a triad of epistaxis, mucocutaneous or visceral telangiectasias, and a family history (Fig. 7). A majority of AVMs (70%) are simple, with a single feeding artery and a single draining vein.[43]

Multiple isolated nodules of 8 mm and smaller in size are typically considered independently as SPNs rather than as multiple nodules caused by a common process.[44] Alternatively, with multiple nodules that are larger than 8 mm in size, the rate of malignancy can be high. In a study of video-assisted thoracoscopic (VATS)-resected lung nodules at an oncology center, 51% of 39 patients with multiple nodules but no history of malignancy at the time of VATS had at least one nodule proven to be malignant.[45] In this population, the investigators demonstrated a 68% rate of malignancy for multiple and solitary nodules of 0.5 cm or smaller in size, and a 70% rate for those between 0.5 and 1 cm in size. The high rate of malignancy in these patients probably reflected the higher risk of cancer in the general population at the investigators' institution, in addition to the inclusion of patients undergoing VATS nodule resection. Clustering of multiple nodules in one area of the lung would suggest a benign over a malignant etiology; however, the presence of a dominant nodule accompanied by smaller satellite nodules can occur with lung cancer.[46]

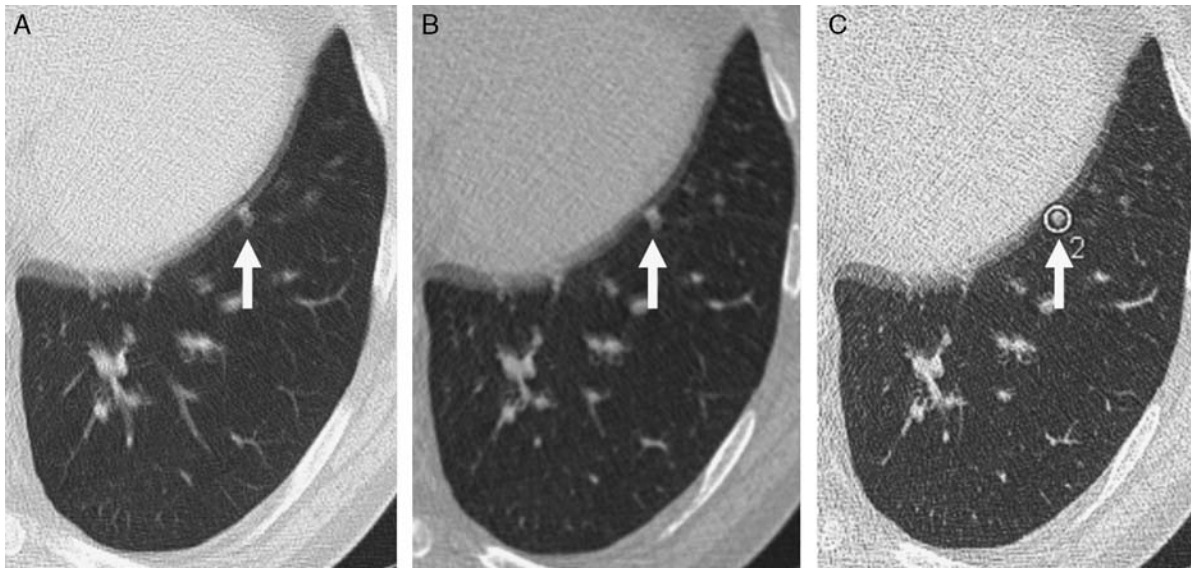

FIGURE 3. CAD detection of overlooked lingular nodule. On 5-mm (A) and 1-mm (B) axial sections, a location adjacent to the heart border and cardiac pulsation artifact in the lung limited the identification of a pulmonary nodule (arrow). C, Axial section with CAD mark (arrow), which was preprocessed on a server and displayed on a clinical PACS workstation, correctly identified the nodule despite the presence of artifact.

Attenuation

Ground-glass attenuation at CT is a characteristic that has been associated with a subset of nodules representing primary lung malignancy, more specifically adenocarcinoma. Anywhere from 20% to 75% of ground-glass nodules are malignant.[34,47] Ground-glass-containing nodules have been termed "subsolid" by some investigators and are pure ground-glass or partly solid, meaning that some soft tissue density is present within the nodule. Persistent pure ground-glass nodules have been associated with primarily bronchioloalveolar carcinomas (BACs). In a study by Kim et al that assessed the cause of persistent pure ground-glass nodules, 40 of 53 (75%) ground-glass nodules were either BAC (36 nodules) or adenocarcinoma (4 nodules). Another cause of ground-glass is nodules atypical adenomatous hyperplasia (AAH), a precursor to adenocarcinoma. AAH comprised 6% of the nodules, while organizing pneumonia or nonspecific fibrosis accounted for 19%. In the study by Kim et al,[47] neoplastic nodules were larger in size with an average diameter of 13 mm, while the AAHs were on average 8 mm. Inflammatory ground-glass nodules had a similar size as their neoplastic counterparts, with a mean diameter of 12 mm. Areas of soft tissue density within ground-glass nodules have been associated with areas of active fibroblastic proliferation and invasive features seen with adenocarcinoma (Fig. 8).[48] The differentiation of AAH, and low-grade BAC is difficult, and nodule sphericity in one investigation was significantly associated with AAH, as opposed to BAC, whereas an internal air bronchogram significantly correlated with BAC.[49] Any increase in density within a persistent ground-glass nodule, with or without associated overall nodule size increase, raises the concern of malignancy and the histologic development of aggressive features. Malignant ground-glass nodules have been described to decrease in size occasionally, usually with increasing density probably related to collapse fibrosis, and therefore continued reassessment by CT of a decreasing nodule may be warranted.[50] Of note, the term BAC will be eliminated from the pathological lexicon and replaced with the term adenocarcinoma to represent tumors with lepidic growth without invasive components.[51] Tumors with invasive components that are 5 mm and smaller will be termed minimally invasive adenocarcinoma. Mixed-attenuation nodules can also represent pulmonary lymphoma, although infrequently (Fig. 6).

The pattern of calcification within an SPN is useful to determine the likelihood of malignancy. Calcification is present within 10.6% of nodules and masses representing lung cancers.[52] Patterns of calcification that raise suspicion for malignancy include eccentric (asymmetric), reticular (linear), punctuate (discrete), and amorphous (indistinct separation between foci of calcification).[53] Eccentric calcification typically occurs when a carcinoma engulfs a preexisting adjacent granuloma. Other patterns of calcification seen in malignant nodules are dystrophic calcification within necrotic areas of tumor and calcification related to mucin production. Benign SPNs calcify in patterns that have been described as central, concentric, popcorn, and diffuse (homogeneous). Prior granulomatous infection is most often associated with central, concentric, or diffuse calcification. Popcorn calcification is seen in hamartomas (Fig. 9). The absence of a benign calcification pattern does not favor a malignant process, as up to 63% of benign nodules lack calcification.[54] Identifiable macroscopic fat within a nodule on MDCT is a fairly characteristic finding of a pulmonary hamartoma,[54] in addition to popcorn calcification. Although rare, other etiologies for pulmonary nodules containing visible fat on CT include solitary liposarcoma metastasis and focus of exogenous lipoid pneumonia (Fig. 10).

Border, Shape, and Location Characteristics

Benign pulmonary nodules most often have a well-defined and smooth border. However, 21% of nodules with a well-defined and smooth border are malignant.[55]

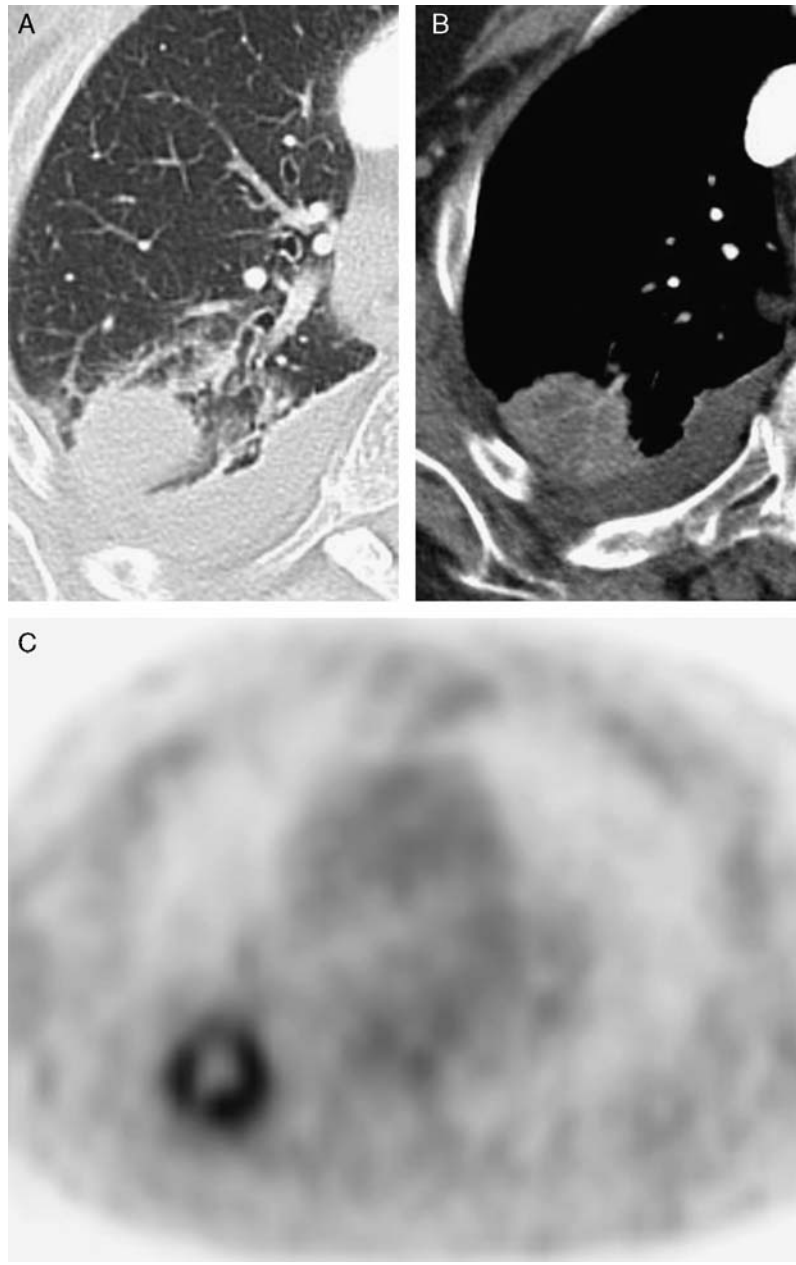

FIGURE 4. Axial chest CT images (A, B) depict a large nodule in the right upper lobe with mild low attenuation centrally and patent vessels. C, PET uptake is present mainly in the periphery of the lesion, suggesting central necrosis. Transthoracic needle biopsy confirmed a focal abscess.

A spiculated pulmonary nodule is most likely to be malignant; however, this may not be a discriminator for subsolid nodules.[47] A lobular border is most often associated with malignant nodules. In the Dutch-Belgian randomized lung cancer screening trial (Nederlands Leuvens Longkanker Screeningsonderzoek), lobular nodules had a higher likelihood for malignancy compared with smooth nodules, and all malignancies were intraparenchymal, without attachment to vessels.[56,57] However, up to 25% of benign nodules also can have a lobular border.[58] For subsolid nodules, morphology (shape, border, and presence of pleural tags) did not differentiate benign etiologies such as interstitial fibrosis from the malignant BAC and adenocarcinoma in an investigation by Kim et al.[47]

Nodules surrounded by a ground-glass halo are nonspecific. The halo can represent either infection (often fungal) or hemorrhage secondary to vasculitis or metastatic disease. Ground-glass halos are more commonly seen in the setting of multiple nodules than with an SPN. When associated with an SPN, the halo sign raises the suspicion for BAC or, uncommonly, parenchymal lymphoma (Fig. 6).[59] A reversed halo sign occurs when a nodule has central ground glass surrounded by soft tissue density.[60] The sign has been described with organizing pneumonia

TABLE 1. Differential Diagnosis of Solitary Pulmonary Nodule

Etiology	Disease
Neoplastic	
Malignant	Primary lung cancer (including adenocarcinoma, squamous cell carcinoma, bronchioloalveolar carcinoma, and small cell carcinoma)
	Metastatic disease (including colon, breast, prostate, testicular, renal cell carcinoma, melanoma, and osteosarcoma)
	Primary carcinoid
	Primary lymphoma
Benign	Hamartoma, neural tumor, fibroma, chondroma
	Arteriovenous malformation
Infectious	Granulomatous (mycobacterial or fungal)
	Bacterial
	Abscess, septic embolus
Noninfectious	Sarcoidosis, Wegener granulomatosis, Rheumatoid arthritis, amyloidosis
	Infarct
	Intrapulmonary lymph node
Congenital	Bronchial atresia
	Intraparenchymal bronchogenic cyst

and other infectious and inflammatory etiologies. With this pattern, nodules are also typically multiple.

Both benign and malignant SPNs can have cavitation and air bronchograms (Fig. 11).[61] Cavitation can occur with infection, vasculitis, primary lung cancer, and metastatic disease. Cavity wall thickness has been investigated as a differentiating characteristic between benign and malignant nodules. In one investigation of cavities on radiographs, cavitary nodules with a wall thickness less than 4 mm were benign in 92% of cases, whereas those with a wall thickness greater than 16 mm were malignant in 95% of cases. Cavitary nodules with walls of intermediate (5 to 15 mm) thickness were malignant 51% of the time.[62] On CT, Honda et al[63] reported that irregularity of the inner cavity wall was significantly more frequent in malignant compared with benign cavities (49% and 26%, respectively). A linear outer cavity wall was significantly more common in benign compared with malignant cavities (32% and 13%, respectively). An outer wall notch was identified more in malignant than in benign cavities (54% and 29%, respectively). Nodule shape also offers predictive value, with an irregular shape having a higher likelihood for malignancy, as compared with round or polygonal nodules.[56] Air bronchograms are frequently seen in focal infections, such as round pneumonia, but occur also in malignancy, such as mucinous adenocarcinoma.

An upper lobe location for a lung nodule increases the possibility that a lesion is lung cancer.[64] However, apical segment nodularity that is small, peripheral, subpleural, and irregular is frequently seen and presumably related

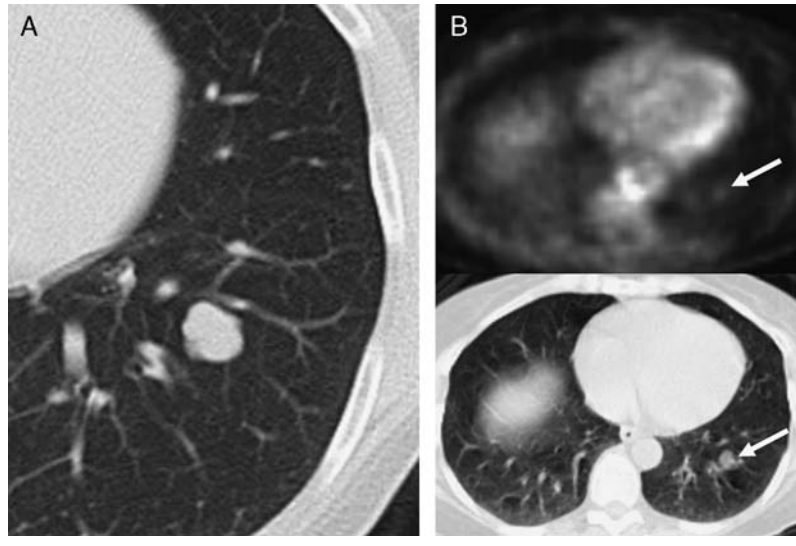

FIGURE 5. Left lower lobe carcinoid. A, Five-millimeter CT section demonstrates a mildly lobulated, ovoid, well-circumscribed nodule in the left lower lobe. B, PET-CT imaging demonstrates mildly increased metabolic activity (standard uptake value, 2.0) corresponding to the nodule (arrow). Surgical resection confirmed a typical carcinoid.

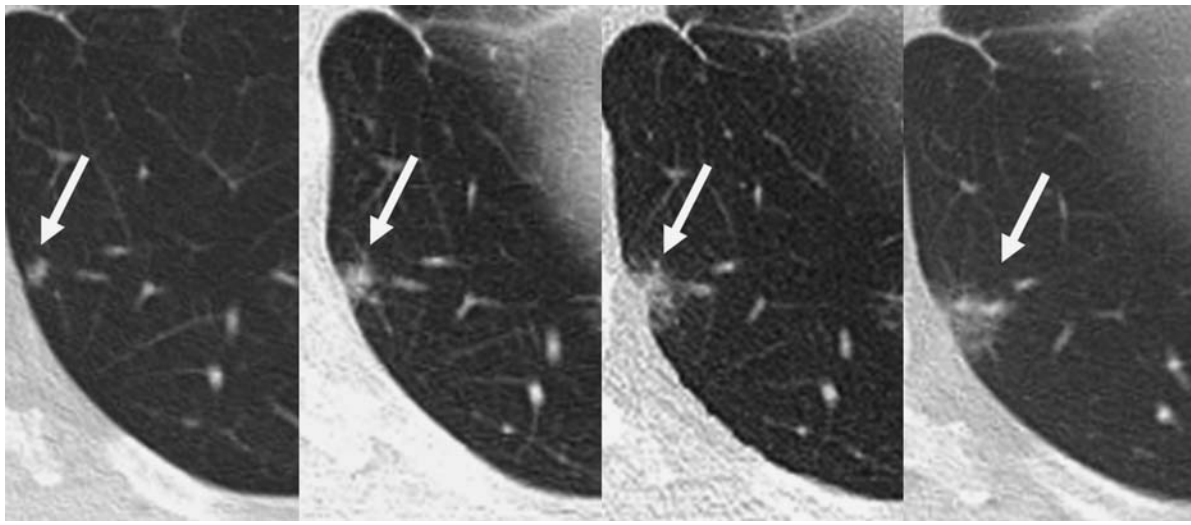

FIGURE 6. Primary pulmonary lymphoma. Slow growth over 5.3 years of a pulmonary nodule (arrows) with solid and ground-glass components, as seen on initial CT (left image), and CTs taken 3 (second from left), 4.5 (second from right), and 5.5 (right image) years later.

to postinflammatory fibrosis.[46] Perifissural densities are frequently small intraparenchymal lymph nodes with low malignant potential, as described in screening populations. These lymph nodes often appear triangular or oval in shape on CT (Fig. 12).[46,65]

Finally, nodule characterization using computer-assisted techniques remains under investigation.[66] The goal for computer assistance is to improve consistency in characterizing nodules and to better predict their etiology and behavior.[67] Continued research in this area may provide greater insight into the predictive value of nodule characteristics.

NODULE VOLUME AND GROWTH ASSESSMENT

Noncalcified subcentimeter pulmonary nodules detected on MDCT are monitored frequently with serial follow-up CT examinations. This is because 18F-FDG-PET, contrast-enhanced CT, and CT-guided percutaneous biopsy are less accurate for evaluating small pulmonary nodules. The follow-up assessment of pulmonary nodules does not only include evaluating for interval size change, but also morphology and attenuation changes.

Follow-up MDCT assessment of SPN size change can be accomplished either qualitatively or quantitatively. The most common technique for quantitative measurement is the manual placement of electronic calipers at the maximum cross-sectional diameter on axial sections. However, Revel et al[68] demonstrated that 2-dimensional CT measurements to evaluate for a size change are not reliable. They found poor intrareader and interreader agreement on 2-dimensional size measurements. In addition, asymmetric growth may not be detected with 2-dimensional measurements. Three-dimensional volumetric measurement techniques have been shown to be more accurate.[69]

Computer-assisted techniques, primarily semiautomated, have been developed for measuring pulmonary nodules in linear dimensions and volumetrically. Some are currently commercially available. Computer-assisted methods have been evaluated for use in the clinical scenarios of nodule characterization and for the surveillance of known malignancy, the latter typically performed according to the Response Assessment Criteria in Solid Tumors and World Health Organization criteria. Schwartz et al[70] reported that measurement of tumor size was more consistent among readers using an automated autocontour technique than electronic calipers. Increasing knowledge of the precision (repeatability) and accuracy (bias) of these techniques has been obtained.[71–73] Computer-based linear and volume measurement methods use similar 3-dimensional nodule analysis technology, with differences being the output obtained.

There are many factors that limit computer-assisted nodule measurement. These include irregular margins, irregular overall shape, adjacent structures, and emphysema. Differences in inspiratory lung volume and cardiac cycle

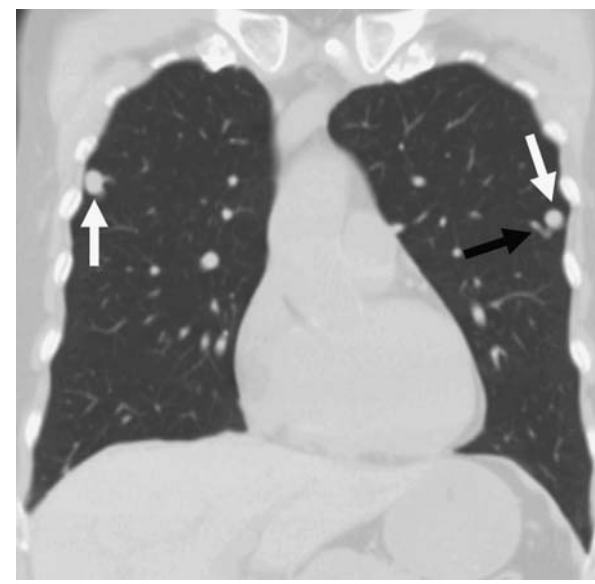

FIGURE 7. Arteriovenous malformations. Coronal maximum projection reconstruction (MPR) shows 2 pulmonary nodules (white arrows) with prominent draining vein, which is shown for the left upper lobe nodule (black arrow).

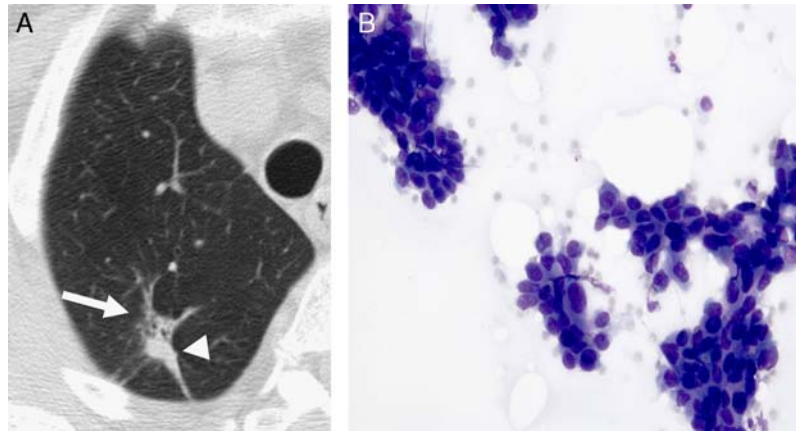

FIGURE 8. Mixed solid and ground-glass pulmonary nodule. A, Axial CT section shows a nodular soft tissue area devoid of air bronchograms (arrowhead) and ground-glass opacity (arrow) that was adenocarcinoma (B) on needle aspiration. The shape of this nodule is polygonal in some portions. The lesion was confirmed by resection as a moderately differentiated adenocarcinoma with a BAC component.

phase also limit the usefulness of computer-assisted nodule measurements when evaluating a follow-up study.[74–79] Border characteristics can affect measurement variability because many techniques rely on segmentation of a nodule's border from adjacent structures, such as vessels, and shape assessment. Difficulty measuring perivascular, spiculated, perifissural, and pleural-based nodules has been reported by some[77–79] but not all investigations.[80] In addition, some studies have shown that different CT doses and reconstruction parameters affect nodule measurement.[80–82] Smaller nodules are associated with greater measurement error given their susceptibility to partial volume effect.[73,80] In addition, measurement precision was shown by Rampinelli et al[83] to change after intravenous contrast administration in patients who underwent multiphase contrast-enhanced CT. A 4% to 6% and 4% to 7% higher median volume was identified for nodules on postcontrast compared with noncontrast images for two different commercial software packages. This occured at all time points for one software program, and at all time points except 30 seconds after contrast for the other program. The investigators postulated that this effect was due to increased attenuation of the nodule's edge that affected nodule segmentation. The particular phase of contrast enhancement was not a significant factor in nodule volume calculation. Therefore, the volume difference may need to be considered when comparing nodule volume measurements from CTs obtained with contrast to those without contrast. Finally, precision of volume measurement has minimally addressed nodules of ground-glass attenuation, with investigation so far primarily in phantom studies and with noncommercial products.[84,85]

Reported precision of volumetric analysis depends on the software program and emphasizes the need to measure nodule volume change with the same program. In an evaluation of 6 semiautomated software programs, De Hoop et al[73] reported the variability of measuring nodule volume on two unenhanced CT scans performed on the same visit in each of 20 patients with pulmonary metastases. Adequate segmentation occurred in 71% to 86% of nodules with a variability of 16.4% to 22.3% (Fig. 13). The investigators noted that there were systemic volume differences among 11 of 15 comparisons of manufacturers. Marchiano et al,[86] using a commercially-available software program, demonstrated a 95% confidence interval for differences in measured volumes in the range of ±27%, meaning a change in 27% of volume was probably a significant change. Rampinelli et al[87] recommended in their study that for their volume assessment method tested, a volume change of greater than 30% for nodules between 5 and 10 mm should be confirmed with another follow-up CT to confirm nodule growth.

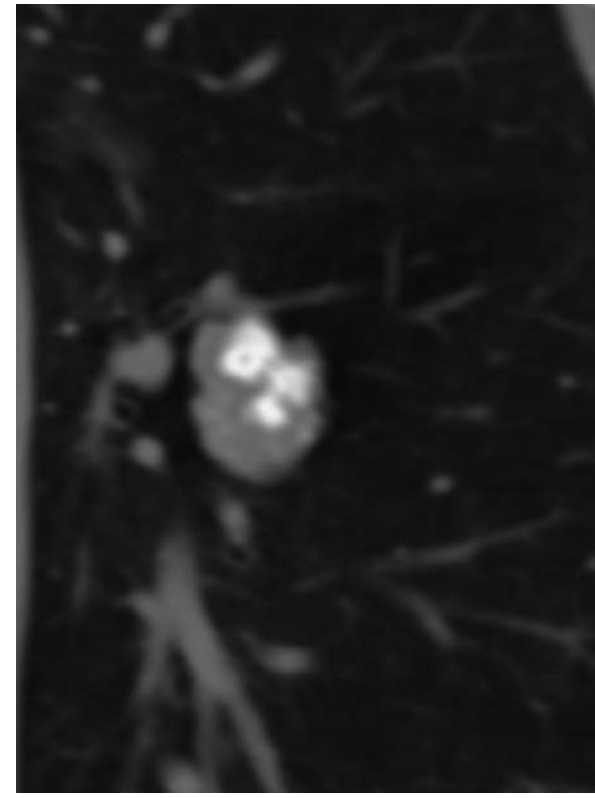

FIGURE 9. Popcorn calcification in a hamartoma displayed on coronal CT reconstruction.

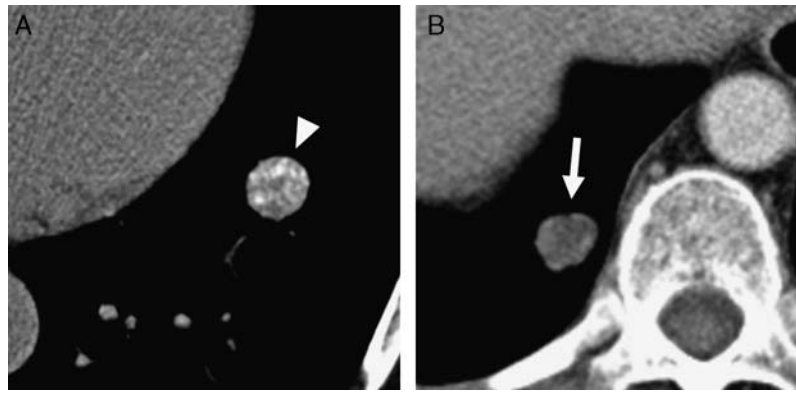

FIGURE 10. Fat-containing nodules. A, Axial CT section viewed under soft tissue settings demonstrates both calcification and macroscopic fat (arrowhead). B, Liposarcoma metastasis also containing macroscopic fat (arrow).

The increase in the volume of a nodule over time has been used as a method to differentiate benign from malignant nodules. Malignant nodules change in volume at a faster rate than persistent benign nodules, which typically remain stable or increase at a slow rate. Nodule growth over time has typically been expressed in terms of volume-doubling time. Malignant nodules generally have volume-doubling times between 20 and 400 days.[88–90] Benign nodules generally have volume-doubling times less than 20 days or more than 450 days. The volume-doubling time for small cell lung cancer is very fast, approximately 30 days, whereas adenocarcinoma of the lung has a volume-doubling time of approximately 180 days, with squamous cell in between.[91] Very rapid doubling times are seen in patients with AIDS- and Epstein-Barr virus-associated lymphoma[92] and overlap with infectious nodules. In addition, neoplasia can have long volume-doubling times. Bronchioloalveolar cell neoplasms can have very long volume-doubling times, on the order of 800 days.[48] It has also been shown that volume-doubling times are an independent prognostic factor for lung cancer patients—independent of N, M, and T status. Shorter doubling times are associated with increased mortality.[93] Bronchial carcinoids can have a doubling time greater than 400 days.[89] For a solid SPN, two-year stability typically indicates a benign lesion. However, stability over two years does not imply a benign lesion when the SPN is subsolid.[46] Therefore, more caution must be exercised when managing an SPN despite two-year size stability.[94]

Volume is not the only finding that changes with nodule growth. Border characteristics and nodule shape can change in the setting of asymmetric growth.[69] Computer-assisted devices can potentially quantify morphologic features associated with malignancy and therefore recognize these changes.[66] However, the mean baseline CT density of solid nodules displayed by an automated program was not shown to differentiate malignant from benign nodules, although the median change in density was significantly different between benign (−0.1 HU) and malignant nodules (12.8 HU).[95] For subsolid nodules, a recent study demonstrated that an increase in nodule mass was determined to be a better indicator of growth than an increase in volume. The mean nodule mass was expressed as the nodule volume multiplied by the mean attenuation in the volume (HU adjusted by adding 1000).[96] In this study, volume was determined manually by observers and was therefore subject to technical factors that affect quantitative evaluation. The role of new measures for the identification of subsolid nodules will be clarified by future investigation.

METABOLIC ACTIVITY ON 18F-FDG-PET

18F-FDG-PET can help differentiate malignant and benign pulmonary nodules. This technique is typically reserved for those that measure 10 mm or greater in size. For nodules greater than 8 mm and less than 10 mm in size, the efficacy of PET is diminished given the number of false negatives and is generally discouraged, except in investigational situations or on a case by case basis.[34] A number of

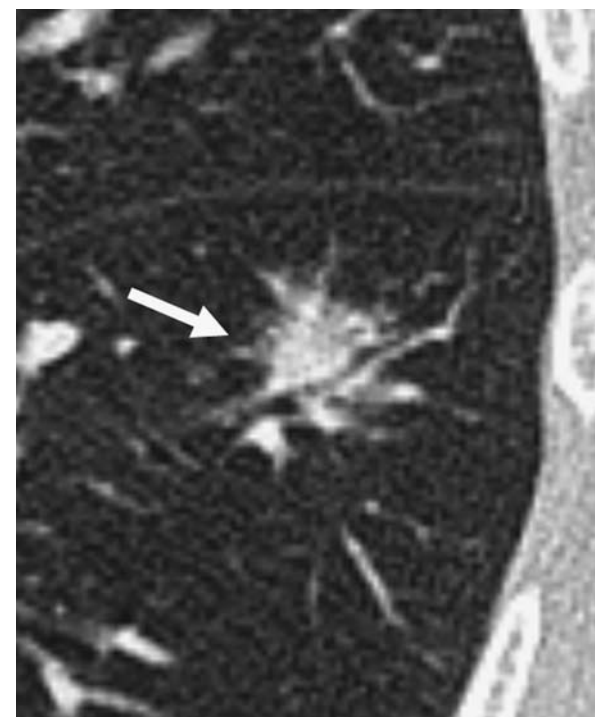

FIGURE 11. Axial CT section shows an air bronchogram within a spiculated soft tissue nodule (arrow) in a low-grade B cell lymphoma of bronchus-associated lymphoid tissue. The air bronchogram can be seen with infection in addition to mucinous adenocarcinoma.

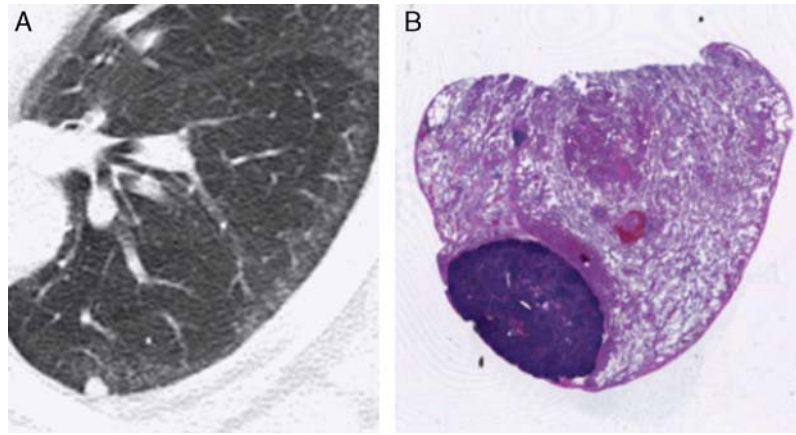

FIGURE 12. Intraparenchymal lymph node (A) CT axial section shows a smoothly marginated, well-circumscribed nodule in the left lower lobe. B, This nodule was an intraparenchymal lymph node on hematoxylin and eosin stain. Pathology courtesy of Herman Yee, MD.

investigations have been published concerning the efficacy of PET. PET has sensitivities on the order of 80% to 100%, with specificities on the order of 40% to 100%. In an analysis by Wahidi et al[35] of 17 published studies, a pooled 87% sensitivity and 83% specificity were reported. Abnormal 18F-FDG accumulation can occur with infectious nodules due to fungi and mycobacteria, sarcoidosis, rheumatoid nodules, and other causes of focal inflammatory lung disease.[34,97] As mentioned, false-negative 18F-FDG-PET results can occur with pulmonary nodules smaller than 10 mm in size. In addition, tumors such as bronchioloalveolar cell carcinoma, well-differentiated adenocarcinoma, and carcinoid can all have low FDG uptake.[97,98] In an investigation of seven carcinoid tumors by Erasmus et al,[99] a total of six tumors (three endobronchial and three parenchymal) had no abnormal FDG uptake (Fig. 5). FDG-PET has been demonstrated to have a high negative predictive value; however, lesions that are

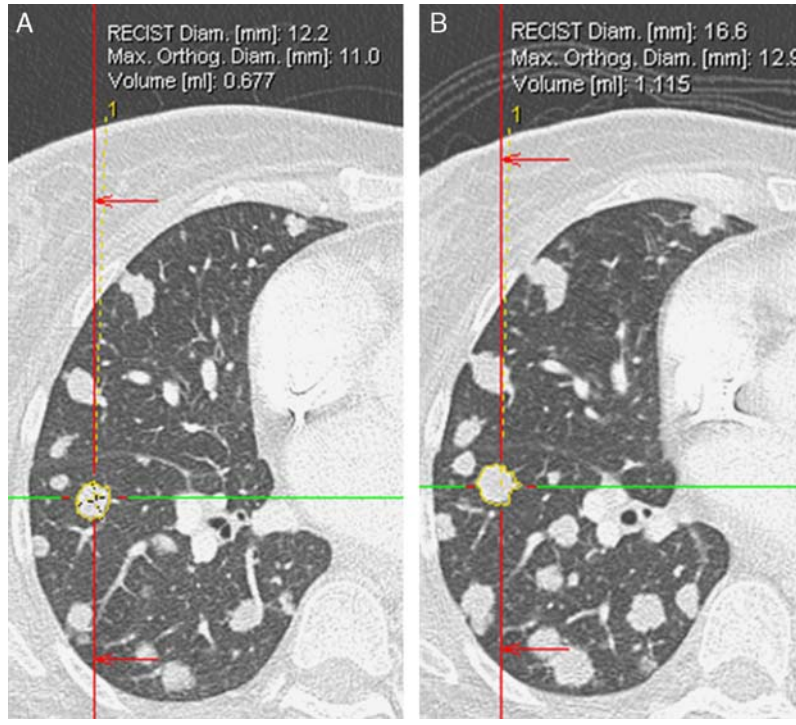

FIGURE 13. Computer-assisted segmentation and measurement of progressive colon metastases. A, Segmented nodule with dimensions on baseline CT examination are shown with a Response Assessment Criteria in Solid Tumors (RECIST) maximal nodule diameter of 12.2 mm and a volume of 0.667 mL. B, Segmentation of nodule on CT scan 2 months later demonstrates a RECIST maximal diameter of 16.6 mm and a volume of 1.115 mL, representing a 36% increase in maximal dimension and a 67% increase in volume.

deemed probably benign are recommended to be followed up by CT to ensure that false-negative PET results are later identified.[34]

NODULE ENHANCEMENT CHARACTERISTICS ON MDCT

CT nodule enhancement is a method that is not frequently used, although it is an option when 18F-FDG PET imaging is not available.[100–102] This technique is less frequently performed given the increasing access to 18F-FDG-PET imaging and the technical expertise required for CT nodule-enhancement studies.[103] Nodules that measure greater than 7 mm and less than 30 mm and lack calcification, cavitation, or ground-glass attenuation can be characterized using this technique. Studied in a multicenter trial, imaging is performed prior to and 1, 2, 3, and 4 minutes after intravenous contrast. The nodule's precontrast attenuation is subtracted from the maximal attenuation after intravenous contrast administration, as measured with a region of interest placed over a majority of the nodule on its largest cross-section in thin-section CT images. A 15-HU or smaller enhancement suggests a benign etiology. To avoid false-negative diagnoses, the investigators for this multicenter study recommended the use of a 10-HU threshold for enhancement and follow-up imaging with CT. The sensitivity and specificity were 98% and 58%, respectively, using a 15 HU threshold. Given the lower specificity of this technique, a greater than 15 HU increase may reflect either malignant or inflammatory disease (Fig. 14).[100]

Nodule enhancement has been investigated with increasing temporal resolution given advances in MDCT technology.[104] In their study using 20-second imaging and 2-dimensional region of interest analysis, Yi et al[104] identified that a 30-HU or greater enhancement had a sensitivity for malignancy of 99%, with a specificity of 54%, positive predictive value of 71%, and negative predictive value of 97%. The analysis of contrast-enhanced data for nodule perfusion can potentially benefit from image-processing techniques including volumetric enhancement analysis and semiquantitative enhancement maps.[105,106] Limited investigation has addressed compartmental modeling with CT, in which enhancement data are analyzed for quantitative measures such as blood volume and volume-transfer constant (K_{trans}) parametric maps.[107] These parameters have been investigated primarily in lung cancer. K_{trans} describes the portion of blood flow that enters the extravascular space. Despite the potential of these techniques, a trade-off exists between the number of imaging time points needed for such techniques and the radiation exposure to the patient. Low-dose techniques with low kVp and reduced mAs and limited coverage imaging have been used to minimize radiation exposure.[107]

Dual-energy (DE) CT imaging was made clinically feasible by the development of dual-source and more recent kVp-switching single-source CT technology.[108] Such technology enables near-simultaneous or simultaneous acquisition both sets of kVp image data. DECT images can now be obtained at similar radiation exposures compared with a traditional single-energy CT acquisition. Image data from both kVps can be fused so that displayed images appear similar to a traditional 120-kVp image (a weighted-average image or "mixed" image). Material-specific images can be created using material decomposition, including an "iodine-enhanced image" that displays the distribution of iodine.[106] The iodine image has at times been referred to as a perfusion image, a misnomer given that the term perfusion implies the enhancement of tissue and blood over time, whereas the iodine image depicts blood volume at a single time point rather than flow.[109] With DECT imaging, an image without the iodine constituents can also be created, termed the virtual nonenhanced or virtual noncontrast image (Fig. 15). Chae et al[110] compared the virtual nonenhanced image for the evaluation of lung nodules to a true noncontrast image and demonstrated good interstudy agreement. The investigators also reported strong agreement between HU values measured on a 3-minute delayed iodine-enhanced image (as a measure of iodine enhancement) and nodule enhancement (difference in HUs between a true precontrast and 3-minute weighted-average images after contrast). The delayed iodine-enhanced CT image HU values had a sensitivity of 92% and a specificity of 70% for malignancy.[111] Although further research is necessary, such techniques may potentially obviate patient radiation by eliminating the need for multiple acquisitions and precontrast imaging.

PULMONARY NODULE MANAGEMENT

The approach to managing pulmonary nodules is multidisciplinary, with input from pulmonologists, surgeons, and radiologists. The evaluation of a pulmonary nodule has been summarized by the American College of Chest Physicians Clinical Practice Guidelines (ACCP).[34] The work up of a nodule includes assessment of a patient's risk for cancer, a weighing of the risks and benefits of evaluation methods, and consideration of patient preferences. Although the complexity of the topic necessitates a full examination of the ACCP guidelines and recommendations, which are given different strengths, a summary of management aspects will be discussed briefly to overview nodule management. Guidelines for the follow-up of subcentimeter pulmonary nodules incidentally detected by MDCT have been issued by the Fleischner Society and integrated into the ACCP guidelines. The workup of nodules that are larger than 10 mm in size provides a greater challenge, in that there are more noninvasive and invasive options for further evaluation.

Patient Risk and Nodule Factors

The ACCP guidelines recommend the qualitative or quantitative assessment of patient risk. Modeling has improved our understanding of risk factors for malignancy[58,112] by determining the likelihood ratios of independent imaging and clinical factors. Specific clinical features determined to be significant predictors of malignancy are age, smoking history, and personal history of cancer 5 or more years prior. Nodule features associated with a higher likelihood of malignancy are size, spiculation, and upper lobe location.[113] A prediction model incorporating these factors was shown to predict the likelihood of malignancy similar to that of experts.[113] The addition of 18F-FDG-PET findings to a Bayesian analysis was shown to increase the effectiveness of the model.[114]

Risks Versus Benefits of Management Options

The likelihood of malignancy is weighed along with the risks to the patient. In terms of initial evaluation of a nodule, comparison with prior imaging is very useful to identify whether a finding is stable, and provides no additional patient risk. If solid and stable for 2 years, the finding is probably benign.[94] If a nodule is ground glass in

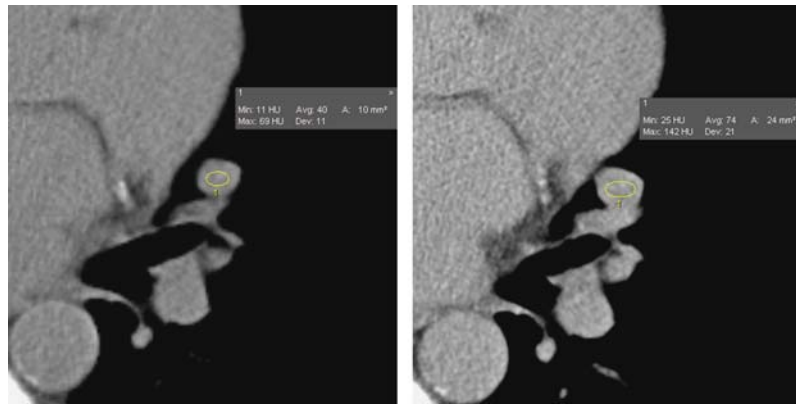

FIGURE 14. CT enhancement study of an enlarging nodule that was PET negative. The average HU measurement increases by 34 HU comparing the precontrast image (left) to the peak enhancement 4 minutes after contrast injection (right).

attenuation on CT, longer follow-up at wider time intervals can be considered given that ground-glass nodule growth has been reported to be slow.[46,115,116] With longer follow-up, the theoretical risk of radiation exposure requires consideration. A reduced-dose, low-mAs imaging technique can be used for follow-up studies to reduce cumulative patient dose.[117] Without prior imaging, CT scan is recommended by the ACCP for indeterminate nodules identified on chest radiography.

The pretest probability of malignancy, related to patient risk and nodule characteristics, can be used to guide management. In the appropriate settings, alternatives to CT follow-up include CT nodule enhancement, FDG-PET, transthoracic or bronchoscopic needle biopsy, and surgical resection. Decision analysis has shown that differences between management strategies are very small, and the chosen approach is typically "a close call."[118] Therefore, the patient is encouraged to actively participate in the decision-making process. An algorithm recommended by the ACCP considers the probability of malignancy when deciding whether to observe, biopsy or resect a nodule.[116] When a very low clinical probability of cancer exists (< 5%) for an SPN that is at least 8 to 10 mm in diameter, ACCP guidelines mention that observation with CT can be performed at 3, 6, 12, and 24 months. Moderate pretest probability patients can undergo further evaluation with FDG-PET and CT nodule enhancement when an SPN is at least 8 to 10 mm in size.[34] However, FDG-PET evaluation of subsolid nodules is prone to false negatives given their low metabolic activity and should not be systematically performed for these nodules. Biopsy remains a possibility for patients with moderate pretest probability, particularly when infection is suspected and when there are discordant FDG-PET findings and patient risk factors. Nodules that are nondiagnostic by biopsy can be observed when not hypermetabolic. However, this may not apply to subsolid lesions given that low FDG-PET activity frequently occurs. When FDG-PET or contrast-enhanced CT is abnormal, the risk of malignancy is increased. The management of such lesions is challenging and depends on a case-by-case analysis considering lesion location and patient comorbidities. Histologic confirmation can be obtained in this scenario via transthoracic biopsy, bronchoscopic biopsy, or thoracoscopic wedge resection by frozen section. Patients with a moderate-to-high rate of malignancy (> 60%) may undergo a surgical diagnosis

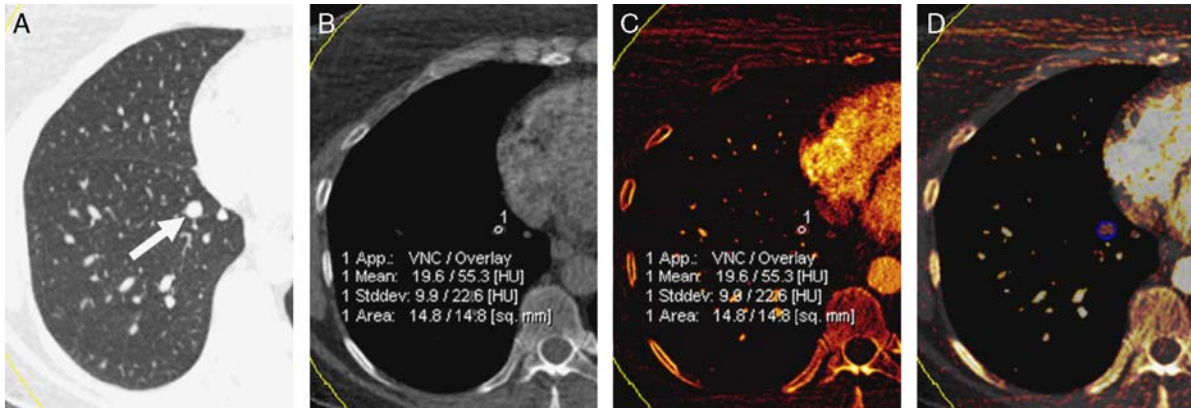

FIGURE 15. Dual-source dual-energy CT in a patient with metastatic melanoma. A, Right lower lobe pulmonary nodule (arrow) on weighted-average image. B and C, After material decomposition, virtual non-contrast (B) and iodine-enhanced images (C) with ROI placed on the nodule demonstrate enhancement of the nodule by 55 HU on iodine-enhanced image. The nodule was 20 HU on the virtual non-contrast image. D, Three-dimensional segmentation of the nodule is possible, as shown on 50/50%-weighted CT/iodine-enhanced image (blue circle). full color online

when the nodule is hypermetabolic on FDG and patient preference is for a definitive diagnostic procedure. Biopsy is recommended prior to any therapy, surgical or nonsurgical.

For small pulmonary nodules less than 8 mm in size, the likelihood of malignancy is very low, on the order of less than 1% in high-risk smokers.[46] The Fleischner Society recommendation for these nodules considers nodule size and patient risk factors for lung cancer. However, nodule multiplicity and distribution are not directly addressed. Relevant patient risk factors include a smoking history, prior malignancy, family history of lung cancer in a first-degree relative, and environmental exposures such as asbestos, radon, and uranium. These recommendations were not designed for application to patients younger than 35 years of age, for those with known extrathoracic malignancy, or cases with unexplained fever.[46] Importantly, the guidelines also do not apply to ground-glass or mixed ground-glass and solid pulmonary nodules. The guidelines suggest that solid pulmonary nodules less than or equal to 4 mm in size need not be followed further in a patient with no risk factors, whereas those individuals with risk factors can have a follow-up in 12 months, with no subsequent evaluation if the nodule is stable. The time interval at which a follow-up CT is performed decreases and the number of follow-up CTs to determine stability increases as nodule size increases, given the positive correlation of nodule size with risk of cancer. Despite the issuance of these guidelines, a lack of coherence in the management of nodules smaller than 10 mm remains,[119,120] which may decrease in the ensuing years as continued dissemination of these guidelines occurs.

Formally proposed management guidelines for ground-glass and subsolid pulmonary nodules have not yet been issued. There are limited options for assessing these lesions noninvasively, other than observation. Transthoracic biopsy can be performed on these lesions.[121] Interim management guidelines have been proposed by Godoy and Naidich.[117] Thin-section evaluation is very useful for identifying any solid components and evaluating the amount of ground-glass attenuation. Given the poorly-defined nature of these nodules, the relationship of the ground glass to the anatomical structures needs to be scrutinized to assess for change. SPNs that are smaller than 5 mm and contain only ground-glass opacity are typically AAH, and it is unclear whether these lesions require follow-up. It has been shown that a small (7%) portion of 5 and 10 mm pure ground-glass opacities can have invasive adenocarinoma features[122]; therefore, CT follow-up in these cases is recommended in 3 to 6 months. Pure ground-glass nodules larger than 10 mm that persist on a 3-month to 6-month follow-up CT are most likely BAC or invasive adenocarcinoma.[117] These lesions are typically resected, particularly if they increase in size or develop solid components.[117] Solid components developing in a ground-glass nodule and representing greater than 50% of the nodule have been associated with increased risk for nodal metastatic disease.[123] Regression of a ground-glass nodule has been described in a small proportion of nodules that are malignant, and therefore follow-up may be warranted to confirm continued size decrease of a ground-glass lesion. The exact length of follow-up time required remains uncertain and must be weighed against the risk of further CT radiation dose. In addition, overdiagnosis of these lesions remains a factor, as there is a question of whether nodules with indolent behavior will affect overall patient survival. Longer intervals, such as one year follow-up, and dose reduction techniques can be used for surveillance of these findings.[117]

SUMMARY

The detection of pulmonary nodules on CT has been aided by advances in technology. The most common etiologies for a malignant SPN are primary lung cancer and metastasis. Infectious granulomas and hamartomas are the most common etiologies for a benign SPN. Diagnostic tools discussed in this review can be used to categorize SPNs as benign, malignant, or indeterminate. Evidence-based clinical guidelines and expert recommendations are available to guide the management of indeterminate SPNs.

REFERENCES

1. Altekruse SF, Kosary CL, Krapcho M, et al. SEER Cancer Statistics Review, 1975-2007. National Cancer Institute: Bethesda, MD. http://seer.cancer.gov/csr/1975_2007/, based on November 2009 SEER data submission. Posted to the SEER web site, 2010.
2. Gould MK, Maclean CC, Kuschner WG, et al. Accuracy of positron emission tomography for diagnosis of pulmonary nodules and mass lesions: a meta-analysis. *JAMA*. 2001; 285:914–924.
3. Shah PK, Austin JH, White CS, et al. Missed non-small cell lung cancer: radiographic findings of potentially resectable lesions evident only in retrospect. *Radiology*. 2003;226: 235–241.
4. Austin JH, Romney BM, Goldsmith LS. Missed bronchogenic carcinoma: radiographic findings in 27 patients with a potentially resectable lesion evident in retrospect. *Radiology*. 1992;182:115–122.
5. Gurney JW. Missed lung cancer at CT: imaging findings in nine patients. *Radiology*. 1996;199:117–122.
6. White CS, Romney BM, Mason AC, et al. Primary carcinoma of the lung overlooked at CT: analysis of findings in 14 patients. *Radiology*. 1996;199:109–115.
7. Ko JP, Rusinek H, Naidich DP, et al. Wavelet compression of low-dose chest CT data: effect on lung nodule detection. *Radiology*. 2003;228:70–75.
8. Kakinuma R, Ohmatsu H, Kaneko M, et al. Detection failures in spiral CT screening for lung cancer: analysis of CT findings. *Radiology*. 1999;212:61–66.
9. Fischbach F, Knollman F, Griesshaber V, et al. Detection of pulmonary nodules by multislice computed tomography: improved detection rate with reduced slice thickness. *Eur Radiol*. 2003;13:2378–2383.
10. Diederich S, Semik M, Lentschig MG, et al. Helical CT of pulmonary nodules in patients with extrathoracic malignancy: CT-surgical correlation. *AJR Am J Roentgenol*. 1999;172: 353–360.
11. Rubin G. Data explosion: the challenge of multidetector row CT. *Eur J Radiol*. 2000;36:74–80.
12. Sakai M, Murayama S, Gibo M, et al. Can Maximum Intensity Projection Images With Multidetector-Row Computed Tomography Help to Differentiate Between the Micronodular Distribution of Focal and Diffuse Infiltrative Lung Diseases? *J Comput Assist Tomogr*. 2005;29:588–591.
13. Gruden JF, Ouanounou S, Tigges S, et al. Incremental benefit of maximum-intensity-projection images on observer detection of small pulmonary nodules revealed by multidetector CT. *AJR Am J Roentgenol*. 2002;179:149–157.
14. Park EA, Goo JM, Lee JW, et al. Efficacy of computer-aided detection system and thin-slab maximum intensity projection technique in the detection of pulmonary nodules in patients with resected metastases. *Invest Radiol*. 2009;44:105–113.
15. Valencia R, Denecke T, Lehmkuhl L, et al. Value of axial and coronal maximum intensity projection (MIP) images in the detection of pulmonary nodules by multislice spiral CT:

comparison with axial 1-mm and 5-mm slices. *Eur Radiol*. 2006;16:325–332.
16. Brown MS, Goldin JG, Suh RD, et al. Lung micronodules: automated method for detection at thin-section CT—initial experience. *Radiology*. 2003;226:256–262.
17. Rubin GD, Lyo JK, Paik DS, et al. Pulmonary nodules on multi-detector row CT scans: performance comparison of radiologists and computer-aided detection. *Radiology*. 2005; 234:274–283.
18. White CS, Pugatch R, Koonce T, et al. Lung nodule CAD software as a second reader: a multicenter study. *Acad Radiol*. 2008;15:326–333.
19. Das M, Muhlenbruch G, Mahnken AH, et al. Small pulmonary nodules: effect of two computer-aided detection systems on radiologist performance. *Radiology*. 2006;241: 564–571.
20. Sahiner B, Chan HP, Hadjiiski LM, et al. Effect of CAD on radiologists' detection of lung nodules on thoracic CT scans: analysis of an observer performance study by nodule size. *Acad Radiol*. 2009;16:1518–1530.
21. Nietert PJ, Ravenel JG, Taylor KK, et al. Influence of nodule detection software on radiologists' confidence in identifying pulmonary nodules with computed tomography. *J Thorac Imaging*. 2010;26:48–53.
22. Zhou J, Chang S, Metaxas DN, et al. Automatic detection and segmentation of ground glass opacity nodules. *Med Image Comput Comput Assist Interv*. 2006;9(Pt 1):784–791.
23. Bastawrous HA, Nitta N, Tsudagawa M. A new CAD system for detecting localized ground glass opacity nodules in lung CT images using cross and coronary section images, in IEEE International Workshop on Medical Measurement and Applications (MeMea). Benevento, Italy. 2006:4–4.
24. Ye X, Lin X, Beddoe G, et al. Efficient computer-aided detection of ground-glass opacity nodules in thoracic CT images. *Conf Proc IEEE Eng Med Biol Soc*. 2007;2007: 4449–4452.
25. Ye X, Lin X, Dehmeshki J, et al. Shape-based computer-aided detection of lung nodules in thoracic CT images. *IEEE Trans Biomed Eng*. 2009;56:1810–1820.
26. Yanagawa M, Honda O, Yoshida S, et al. Commercially available computer-aided detection system for pulmonary nodules on thin-section images using 64 detectors-row CT: preliminary study of 48 cases. *Acad Radiol*. 2009;16:924–933.
27. Beigelman-Aubry C, Hill C, Boulanger X, et al. Evaluation of a computer aided detection system for lung nodules with ground glass opacity component on multidetector-row CT. *J Radiol*. 2009;90:1843–1849.
28. Betke M, Hong H, Thomas D, et al. Landmark detection in the chest and registration of lung surfaces with an application to nodule registration. *Med Image Anal*. 2003;7:265–281.
29. Sun S, Rubin GD, Paik D, et al. Registration of lung nodules using a semi-rigid model: method and preliminary results. *Med Phys*. 2007;34:613–626.
30. Tao C, Gierada DS, Zhu F, et al. Automated matching of pulmonary nodules: evaluation in serial screening chest CT. *American Journal of Roentgenology*. 2009;192:624–628.
31. Lee KW, Kim M, Gierada DS, et al. Performance of a computer-aided program for automated matching of metastatic pulmonary nodules detected on follow-up chest CT. *AJR Am J Roentgenol*. 2007;189:1077–1081.
32. Beyer F, Wormanns D, Novak C, et al. Clinical evaluation of a software for automated localization of lung nodules at follow-up CT examinations. *Rofo*. 2004;176:829–836.
33. Ost D, Fein AM, Feinsilver SH. Clinical practice: the solitary pulmonary nodule. *N Engl J Med*. 2003;348:2535–2542.
34. Gould MK, Fletcher J, Iannettoni MD, et al. Evaluation of patients with pulmonary nodules: when is it lung cancer? ACCP evidence-based clinical practice guidelines (2nd edition). *Chest*. 2007;132(3_suppl):108S–130S.
35. Wahidi MM, Govert JA, Goudar RK, et al. Evidence for the treatment of patients with pulmonary nodules: when is it lung cancer? ACCP evidence-based clinical practice guidelines (2nd edition). *Chest*. 2007;132(3 suppl):94S–107S.
36. Libby DM, Smith JP, Altorki NK, et al. Managing the small pulmonary nodule discovered by CT. *Chest*. 2004;125: 1522–1529.
37. Travis WD. Pathology of lung cancer. *Clin Chest Med*. 2002; 23:65–81, viii.
38. Gephardt GN, Grady KJ, Ahmad M, et al. Peripheral small cell undifferentiated carcinoma of the lung: clinicopathologic features of 17 cases. *Cancer*. 1988;61:1002–1008.
39. Chong S, Lee KS, Chung MJ, et al. Neuroendocrine tumors of the lung: clinical, pathologic, and imaging findings. *Radiographics*. 2006;26:41–57.
40. Rosado de Christenson ML, Abbott GF, Kirejczyk WM, et al. From the Archives of the AFIP. Thoracic Carcinoids: Radiologic-Pathologic Correlation. *Radiographics*. 1999;19: 707–736.
41. Cordier JF, Valeyre D, Guillevin L, et al. Pulmonary Wegener's granulomatosis: a clinical and imaging study of 77 cases. *Chest*. 1990;97:906–912.
42. Ginsberg MS, Griff SK, Go BD, et al. Pulmonary nodules resected at video-assisted thoracoscopic surgery: etiology in 426 patients. *Radiology*. 1999;213:277–282.
43. Maldonado JA, Henry T, Gutiérrez FR. Congenital thoracic vascular anomalies. *Radiol Clin N Am*. 2010;48:85–115.
44. Henschke CI, McCauley DI, Yankelevitz DF, et al. Early Lung Cancer Action Project: overall design and findings from baseline screening. *Lancet*. 1999;354:99–105.
45. Ginsberg MS, Griff SK, Go BD, et al. Pulmonary nodules resected at video-assisted thoracoscopic surgery: etiology in 426 patients. *Radiology*. 1999;213:277–282.
46. MacMahon H, Austin JH, Gamsu G, et al. Guidelines for management of small pulmonary nodules detected on CT scans: a statement from the Fleischner Society. *Radiology*. 2005;237:395–400.
47. Kim HY, Shim YM, Lee KS, et al. Persistent pulmonary nodular ground-glass opacity at thin-section CT: histopathologic comparisons. *Radiology*. 2007;245:267–275.
48. Aoki T, Watanabe H, Nakamura K, et al. Evolution of peripheral lung adenocarcinomas: CT findings correlated with histology and tumor doubling time. *AJR Am J Roentgenol*. 2000;174:763–768.
49. Oda S, Awai K, Liu D, et al. Ground-glass opacities on thin-section helical CT: differentiation between bronchioloalveolar carcinoma and atypical adenomatous hyperplasia. *AJR Am J Roentgenol*. 2008;190:1363–1368.
50. Kakinuma R, Ohmatsu H, Kaneko M, et al. Progression of focal pure ground-glass opacity detected by low-dose helical computed tomography screening for lung cancer. *J Comput Assist Tomogr*. 2004;28:17–23.
51. Travis WD, Brambilla E, Noguchi M, et al. International Association for the Study of Lung Cancer/American Thoracic Society/European Respiratory Society International Multidisciplinary Classification of Lung Adenocarcinoma. *J Thorac Oncol*. 2011;6:244–285.
52. Grewal RG, Austin JH. CT demonstration of calcification in carcinoma of the lung. *J Comput Assist Tomogr*. 1994;18:867–871.
53. Mahoney M, Shipley RT, Corcoran HL, et al. CT demonstration of calcification in carcinoma of the lung. *Am J Roentgenol*. 1990;154:255–258.
54. Siegelman SS, Khouri NF, Leo FP, et al. Solitary pulmonary nodules: CT assessment. *Radiology*. 1986;160:307–312.
55. Siegelman SS, Zerhouni EA, Leo FP, et al. CT of the solitary pulmonary nodule. *AJR Am J Roentgenol*. 1980;135:1–13.
56. Xu DM, van Klaveren RJ, de Bock GH, et al. Limited value of shape, margin and CT density in the discrimination between benign and malignant screen detected solid pulmonary nodules of the NELSON trial. *Eur J Radiol*. 2008; 68:347–352.
57. Xu DM, van der Zaag-Loonen HJ, Oudkerk M, et al. Smooth or attached solid indeterminate nodules detected at baseline

CT screening in the NELSON study: cancer risk during 1 year of follow-up. *Radiology*. 2009;250:264–272.
58. Gurney JW, Lyddon DM, McKay JA. Determining the likelihood of malignancy in solitary pulmonary nodules with Bayesian analysis. Part II. Application. *Radiology*. 1993;186: 415–422.
59. Lee YR, Choi YW, Lee KJ, et al. CT halo sign: the spectrum of pulmonary diseases. *Br J Radiol*. 2005;78:862–865.
60. Kim SJ, Lee KS, Ryu YH, et al. Reversed halo sign on high-resolution CT of cryptogenic organizing pneumonia: diagnostic implications. *Am J Roentgenol*. 2003;180:1251–1254.
61. Lee KS, Kim Y, Han J, et al. Bronchioloalveolar carcinoma: clinical, histopathologic, and radiologic findings. *Radiographics*. 1997;17:1345–1357.
62. Woodring J, Fried A, Chuang V. Solitary cavities of the lung: diagnostic implications of cavity wall thickness. *Am J Roentgenol*. 1980;135:1269–1271.
63. Honda O, Tsubamoto M, Inoue A, et al. Pulmonary cavitary nodules on computed tomography: differentiation of malignancy and benignancy. *J Comput Assist Tomogr*. 2007;31: 943–949.
64. Byers TE, Vena JE, Rzepka TF. Predilection of lung cancer for the upper lobes: an epidemiologic inquiry. *J Natl Cancer Inst*. 1984;72:1271–1275.
65. Ahn MI, Gleeson TG, Chan IH, et al. Perifissural nodules seen at CT screening for lung cancer. *Radiology*. 2010;254:949–956.
66. Way TW, Sahiner B, Chan HP, et al. Computer-aided diagnosis of pulmonary nodules on CT scans: improvement of classification performance with nodule surface features. *Med Phys*. 2009;36:3086–3098.
67. Iwano S, Nakamura T, Kamioka Y, et al. Computer-aided differentiation of malignant from benign solitary pulmonary nodules imaged by high-resolution CT. *Comput Med Imaging Graph*. 2008;32:416–422.
68. Revel MP, Bissery A, Bienvenu M, et al. Are two-dimensional CT measurements of small noncalcified pulmonary nodules reliable? *Radiology*. 2004;231:453–458.
69. Yankelevitz DF, Reeves AP, Kostis WJ, et al. Small pulmonary nodules: volumetrically determined growth rates based on CT evaluation. *Radiology*. 2000;217:251–256.
70. Schwartz LH, Ginsberg MS, DeCorato D, et al. Evaluation of tumor measurements in oncology: use of film-based and electronic techniques. *J Clin Oncol*. 2000;18:2179–2184.
71. Yankelevitz DF, Gupta R, Zhao B, et al. Small pulmonary nodules: evaluation with repeat CT—preliminary experience. *Radiology*. 1999;212:561–566.
72. Marchiano A, Calabro E, Civelli E, et al., Pulmonary nodules: volume repeatability at multidetector CT lung cancer screening. *Radiology*. 2009;251:919–925.
73. De Hoop B, Gietema H, van Ginneken B, et al. A comparison of six software packages for evaluation of solid lung nodules using semi-automated volumetry: what is the minimum increase in size to detect growth in repeated CT examinations. *Eur Radiol*. 2008;19:800–808.
74. Petkovska I, Brown MS, Goldin JG, et al. The effect of lung volume on nodule size on CT. *Acad Radiol*. 2007;14:476–485.
75. Gietema HA, Schaefer-Prokop CM, Mali WP, et al. Pulmonary nodules: Interscan variability of semiautomated volume measurements with multisection CT—influence of inspiration level, nodule size, and segmentation performance. *Radiology*. 2007;245:888–894.
76. Boll DT, Gilkeson RC, Fleiter TR, et al. Volumetric assessment of pulmonary nodules with ECG-gated MDCT. *AJR Am J Roentgenol*. 2004;183:1217–1223.
77. Gietema HA, Wang Y, Xu D, et al. Pulmonary nodules detected at lung cancer screening: interobserver variability of semiautomated volume measurements. *Radiology*. 2006;241: 251–257.
78. Wang Y, de Bock GH, van Klaveren RJ, et al. Volumetric measurement of pulmonary nodules at low-dose chest CT: effect of reconstruction setting on measurement variability. *Eur Radiol*. 2010;20:1180–1187.
79. Ko JP, Marcus R, Bomsztyk E, et al. Effect of blood vessels on measurement of nodule volume in a chest phantom. *Radiology*. 2006;239:79–85.
80. Rampinelli C, De Fiori E, Raimondi S, et al. In vivo repeatability of automated volume calculations of small pulmonary nodules with CT. *AJR Am J Roentgenol*. 2009; 192:1657–1661.
81. Hein PA, Romano VC, Rogalla P, et al. Variability of semiautomated lung nodule volumetry on ultralow-dose CT: comparison with nodule volumetry on standard-dose CT. *J Digit Imaging*. 2008;23:8–17.
82. Hein PA, Romano VC, Rogalla P, et al. Linear and volume measurements of pulmonary nodules at different CT dose levels-intrascan and interscan analysis. *RoFo*. 2009;181:24–31.
83. Rampinelli C, Raimondi S, Padrenostro M, et al. Pulmonary nodules: contrast-enhanced volumetric variation at different CT scan delays. *AJR Am J Roentgenol*. 2010;195:149–154.
84. Oda S, Awai K, Murao K, et al. Computer-aided volumetry of pulmonary nodules exhibiting ground-glass opacity at MDCT. *AJR Am J Roentgenol*. 2010;194:398–406.
85. Iwano S, Okada T, Koike W, et al. Semi-automatic volumetric measurement of lung cancer using multi-detector CT effects of nodule characteristics. *Acad Radiol*. 2009; 16:1179–1186.
86. Marchiano A, Calabro E, Civelli E, et al. Pulmonary nodules: volume repeatability at multidetector CT lung cancer screening. *Radiology*. 2009;251:919–925.
87. Rampinelli C, De Fiori E, Raimondi S, et al. In vivo repeatability of automated volume calculations of small pulmonary nodules with CT. *Am J Roentgenol*. 2009;192:1657–1661.
88. Nathan MH, Collins VP, Adams RA. Differentiation of benign and malignant pulmonary nodules by growth rate. *Radiology*. 1962;79:221–232.
89. Collins VP, Loeffler RK, Tivey H. Observations on growth rates of human tumors. *Am J Roentgenol*. 1956;76:988–1000.
90. Steele JD, Buell P. Asymptomatic solitary pulmonary nodules. Host survival, tumor size, and growth rate. *J Thorac Cardiovasc Surg*. 1973;65:140–151.
91. Winer-Muram HT, Jennings SG, Tarver RD, et al. Volumetric growth rate of stage I lung cancer prior to treatment: serial CT scanning. *Radiology*. 2002;223:798–805.
92. Girvin F, Ko J. Pulmonary nodules: detection, assessment, and CAD. *Am J Roentgenol*. 2008;191:1057–1069.
93. Usuda K, Saito Y, Sagawa M, et al. Tumor doubling time and prognostic assessment of patients with primary lung cancer. *Cancer*. 1994;74:2239–2244.
94. Yankelevitz D, Henschke C. Does 2-year stability imply that pulmonary nodules are benign? *Am J Roentgenol*. 1997;168:325–328.
95. Xu DM, van Klaveren RJ, de Bock GH, et al. Role of baseline nodule density and changes in density and nodule features in the discrimination between benign and malignant solid indeterminate pulmonary nodules. *Eur J Radiol*. 2009; 70:492–498.
96. De Hoop B, Gietema H, van de Vorst S, et al. Pulmonary ground-glass nodules: increase in mass as an early indicator of growth. *Radiology*. 2010;255:199–206.
97. Vansteenkiste JF, Stroobants SS. PET scan in lung cancer: current recommendations and innovation. *J Thorac Oncol*. 2006;1:71–73.
98. Goudarzi B, Jacene HA, Wahl RL. Diagnosis and differentiation of bronchioloalveolar carcinoma from adenocarcinoma with bronchioloalveolar components with metabolic and anatomic characteristics using PET/CT. *J Nucl Med*. 2008;49:1585–1592.
99. Erasmus JJ, et al. Evaluation of primary pulmonary carcinoid tumors using FDG PET. *AJR Am J Roentgenol*. 1998;170: 1369–1373.

100. Swensen SJ, Viggiano RW, Midthun DE, et al. Lung nodule enhancement at CT: multicenter study. *Radiology*. 2000; 214:73–80.
101. Swensen SJ, Brown LR, Colby TV, et al. Lung nodule enhancement at CT: prospective findings. *Radiology*. 1996;201:447–455.
102. Yi CA, Lee KS, Kim BT, et al. Tissue characterization of solitary pulmonary nodule: comparative study between helical dynamic CT and integrated PET/CT. *J Nucl Med*. 2006;47: 443–450.
103. Christensen JA, Nathan MA, Mullan BP, et al. Characterization of the solitary pulmonary nodule: 18F-FDG PET versus nodule-enhancement CT 10.2214/AJR.05.1166. *Am J Roentgenol*. 2006;187:1361–1367.
104. Yi CA, Lee KS, Kim EA, et al. Solitary pulmonary nodules: dynamic enhanced multi-detector row CT study and comparison with vascular endothelial growth factor and microvessel density. *Radiology*. 2004;233:191–199.
105. Li Y, Yang ZG, Chen TW, et al. First-pass perfusion imaging of solitary pulmonary nodules with 64-detector row CT: comparison of perfusion parameters of malignant and benign lesions. *Br J Radiol*. 2010;83:785–790.
106. Petkovska I, Shah SK, McNitt-Gray MF, et al. Pulmonary nodule characterization: a comparison of conventional with quantitative and visual semi-quantitative analyses using contrast enhancement maps. *Eur J Radiol*. 2006;59:244–252.
107. Tacelli N, Remy-Jardin M, Copin MC, et al. Assessment of non-small cell lung cancer perfusion: pathologic-CT correlation in 15 patients. *Radiology*. 2010;257:863–871.
108. Johnson TR, Krauss B, Sedlmair M, et al. Material differentiation by dual energy CT: initial experience. *Eur Radiol*. 2007;17:1510–1517.
109. Remy-Jardin M, Faivre JB, Pontana F, et al. Thoracic applications of dual energy. *Radiol Clin N Am*. 2009;48: 193–205.
110. Chae EJ, Song JW, Seo JB, et al. Clinical utility of dual-energy CT in the evaluation of solitary pulmonary nodules: initial experience. *Radiology*. 2008;249:671–681.
111. Kang MJ, Park CM, Lee CH, et al. Dual energy CT: clinical applications in various pulmonary diseases. *Radiographics*. 2010;30:685–698.
112. Swensen SJ, Silverstein MD, Edell ES, et al. Solitary pulmonary nodules: clinical prediction model versus physicians. *Mayo Clin Proc*. 1999;74:319–329.
113. Swensen SJ, Silverstein MD, Ilstrup DM, et al. The probability of malignancy in solitary pulmonary nodules. Application to small radiologically indeterminate nodules. *Arch Intern Med*. 1997;157:849–855.
114. Dewan NA, Shehan CJ, Reeb SD, et al. Likelihood of malignancy in a solitary pulmonary nodule: comparison of Bayesian analysis and results of FDG-PET scan. *Chest*. 1997;112:416–422.
115. Hasegawa M, Sone S, Takashima S, et al. Growth rate of small lung cancers detected on mass CT screening. *Br J Radiol*. 2000;73:1252–1259.
116. Gould MK, Fletcher J, Iannettoni MD, et al. Evaluation of patients with pulmonary nodules: when is it lung cancer? *Chest*. 2007;132(3 suppl):108S–130S.
117. Godoy MC, Naidich DP. Subsolid pulmonary nodules and the spectrum of peripheral adenocarcinomas of the lung: recommended interim guidelines for assessment and management. *Radiology*. 2009;253:606–622.
118. Cummings SR, Lillington GA, Richard RJ. Managing solitary pulmonary nodules. The choice of strategy is a "close call". *Am Rev Respir Dis*. 1986;134:453–460.
119. Esmaili A, Munden RF, Mohammed TL. Small pulmonary nodule management: a survey of the Members of the Society of Thoracic Radiology with Comparison to the Fleischner Society Guidelines. *J Thorac Imaging*. 2011;26:27–31.
120. Prosch H, Strasser G, Oschatz E, et al. Management of patients with small pulmonary nodules: a survey of radiologists, pulmonologists, and thoracic surgeons. *Am J Roentgenol*. 2006;187:143–148.
121. Kim TJ, Lee JH, Lee CT, et al. Diagnostic accuracy of CT-guided core biopsy of ground-glass opacity pulmonary lesions. *Am J Roentgenol*. 2008;190:234–239.
122. Nakata M, Saeki H, Takata I, et al. Focal ground-glass opacity detected by low-dose helical CT. *Chest*. 2002;121: 1464–1467.
123. Vazquez M, Carter D, Brambilla E, et al. Solitary and multiple resected adenocarcinomas after CT screening for lung cancer: histopathologic features and their prognostic implications. *Lung Cancer*. 2009;64:148–154.

